Supporting Information (SI) on

Influence of aqueous sulfide on speciation of U(VI) adsorbed to nano-magnetite

Yubing Sun,[a] Jianhui Lan,[b] Mengxue Li,[c] Wei Hu,[c] Haibo Liu,[c] Gang Song,[d] Diyun Chen,[d] Weiqun Shi,[b*] Xiangke Wang[a*]

[a] *School of Environment and Chemical Engineering, North China Electric Power University, Beijing 102206, P.R. China*

[b] *Laboratory of Nuclear Energy Chemistry and Key Laboratory for Biomedical Effects of Nanomaterials and Nanosafety, Institute of High Energy Physics, Chinese Academy of Sciences, Beijing, 100049, China.*

[c] *School of Resources and Environmental Engineering, Hefei University of Technology, Hefei, 230009, P. R. China*

[d] *Guangdong Provincial Key Laboratory of Radionuclides Pollution Control and Resources，Guangzhou 510006, China* Corresponding Author

* E-mail: shiwq@ihep.ac.cn (W. Shi); xkwang@ncepu.edu.cn (X. Wang)

sunyb@ipp.ac.cn (Y. Sun); lanjh@ihep.ac.cn (J. Lan); 352198925@qq.com (M. Li); 1617359931@qq.com (W. Hu); liuhaibosky116@hfut.edu.cn (H. Liu); songg2005@126.com (G. Song); cdy@gzhu.edu.cn (D. Chen).

Supplemental Information, 11 pages with 7 Figures and 2 Tables

Synthesis of nano-magnetite

Nano-magnetite was synthesized by chemical precipitation of Fe^{2+} and Fe^{3+} under basic conditions, which can be depicted as Eqn. (S1):

$$Fe^{2+} + Fe^{3+} + 8OH^- = Fe_3O_4\downarrow + 4H_2O \qquad (S1)$$

Typically, 0.92 g $FeCl_3 \cdot 6H_2O$ and 0.52 g $FeSO_4 \cdot 7H_2O$ were added to 400 mL DI water at room temperature under N_2 conditions, and then NH4OH solution was titrated to pH 10.0. The suspensions were washed with DI water several times.

The calculation of U(VI) reduction (Ured)

The amount of U(VI) reduction (Ured) was calculated by the difference of adsorbed U(VI) and extracted U(VI) using Na_2CO_3 solution.[1] Briefly, 6 mL of 0.2 mol/L Na_2CO_3 solution was added into the wet paste after reaction. The suspension was reacted for 30 min under vigorous stirring and glovebox conditions. After centrifugation at 6000 rpm for 30 min, the amount of extracted U(VI) was detected by kinetic-phosphorescence-analyzer (KPA-11, Richland, USA).

Detection of dissolved Fe(II) and Fe(III)

The concentration of dissolved Fe(II) and Fe(III) was demonstrated by spectrophotometric method. Briefly, 2 mL of 0.15 % phenanthroline solution and 5 mL HAc-NaAc buffering solution were added into 2 mL of supernatant after reaction, then 1 mL of 10 % hydroxylamine hydrochloride (detection of Fe(II) was not added) was added during the measurement of Fe(III) concentration, and mixtures were diluted to 25 mL and were aged for 10 min. The concentrations were detected by DR3900 UV-VIS spectrophotometer (HACH, USA) at 510 nm.

Characterization of nano-magnetite

The characterizations of nano-magnetite were provided such as TEM, XPS, TGA and magnetization technique. The morphology of nano-magnetite was conducted by TEM (Titan ™ G2 60-300, Hitachi, Japan). The spectra of O 1s XPS spectra were conducted XPS spectrometer (Kratos Axis Ultra) equipped with a monochromatic Al-Kα source and charge compensation system at 40 eV and sweep steps of 0.05 eV. TGA was conducted by using a Shimadzu TGA-50 thermogravimetric analyzer with a air rate of 50 ml/min. The magnetization curve of nano-magnetite was measured by using a model 155 vibrating sample magnetometer at room temperature over the ranging from -20 to 20 kOe.

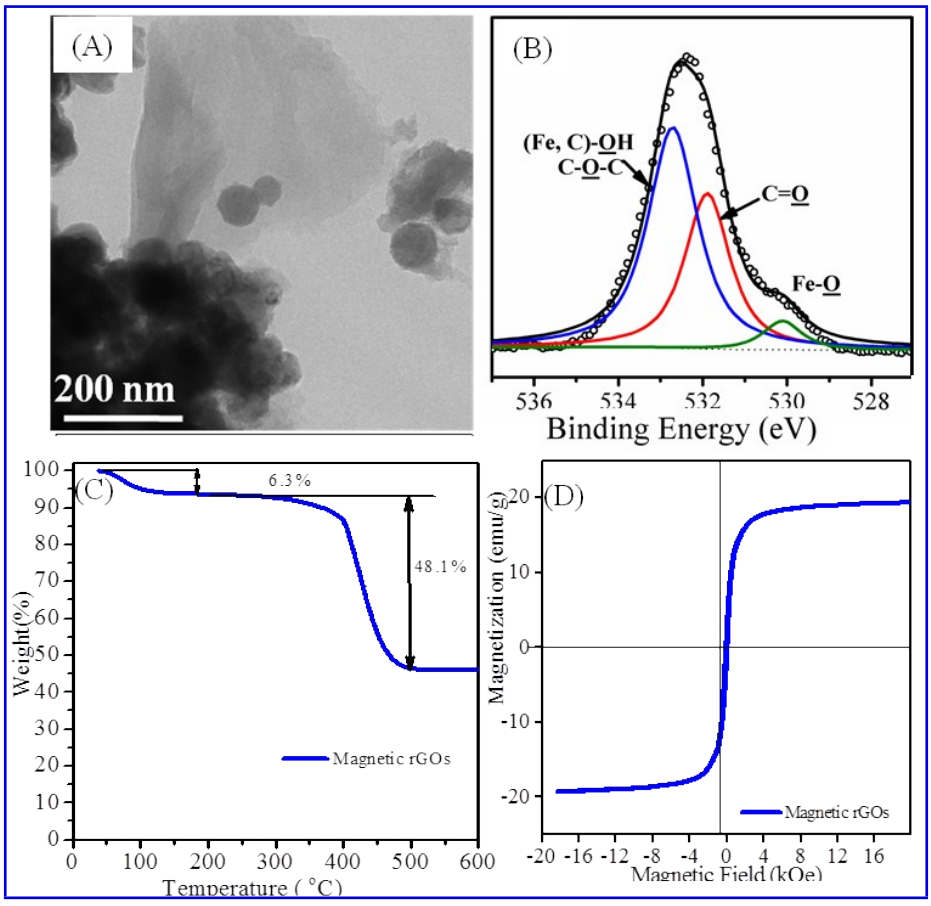

Figure S1 Characterization of nano-magnetite, A: TEM; B: XPS; C: TGA; D: magnetization

Batch adsorption experiments

All experiments were conducted in a glovebox at 293 K. Briefly, 2.5 mg nano-magnetite was added into 5 mL of 10.0 mg/L U(VI) solution with 0.01 mol/L $NaClO_4$ solutions, and then value of pH was adjusted to 4.0 and then reacted 24 h in glovebox conditions. The wet paste of solid was collected after centrifugation it at 6000 rpm for 10 min. The effect of polycarbonate centrifuge tubes was conducted by the blank experiments. Briefly, 5 mL of 10.0 mg/L U(VI) solution with 0.01 mol/L $NaClO_4$ solutions was added into 10 mL polycarbonate centrifuge tubes without nano-magnetite, and then value of pH was adjusted to 4.0 and then reacted 24 h in glovebox conditions. The wet paste of solid was collected after centrifugation it at 6000 rpm for 10 min. The results revealed the no effect of polycarbonate centrifuge tubes on U(VI) adsorption. The adsorption results indicated that adsorption rate of U(VI) significantly increased with increasing reaction time. Approximate 95 % of U(VI) was absorbed by nano-magnetite at reaction time of 3 h.

Preparation of samples for XANES and EXAFS analysis

The samples for uranium XANES and EXAFS spectra were prepared in a glovebox (95 % N_2 + 5 % H_2) at 293 K. Typical, 0.01 mol/L $NaClO_4$ and $UO_2(NO_3)_2$ solution were pre-equilibrated for 24 h, and then solution was added into nano-magnetite under vigorous stirring conditions. After adsorption equilibrium (24 h), the Na_2S solution was added into suspensions at different pH and reaction times. After centrifugation at 9800 rpm for 30 min, wet pastes were sealed in Teflon sample holders under anaerobic conditions. It is reported that U redox states (such as U(IV),

U(V) and U(VI)) can be effectively detected by M_4-edge high energy resolution XANES method at relatively low (1000 ppm) total U concentrations. The high resolution EXAFS spectra were obtained by using spherical bent crystal analyzer in fluorescence mode. Briefly, sample, spherical bent crystal analyzer (radius of curvature, 182 mm) and 32-element Ge detector were located on the geometrical structure of Rowland circle. The samples were irradiated with a beam of X-rays at 45º and then the fluorescence emitted from sample was captured by spherical bent crystal analyzer.

The values of energies (ΔE^0) were fixed to decrease the degree of freedom during the data fitting. The goodness of fit between the experimental and theoretical spectrum was evaluated by R-factor (a least squares residual). Briefly, an initial fit for each shell of atoms was conducted by altering the type of shell and coordination numbers. Then the best fits were obtained by iteratively adjusting bonding distance and Debye-Waller factor at the 1 % significance level. The non-integral CN was finally obtained due to the average information of coordination sites. The accuracies of bonding distance were determined ± 0.05 Å.

Theoretical calculations

All density functional theory (DFT) calculations were performed by using the Vienna ab initio Simulation Package (VASP).[2, 3] The projector augmented wave (PAW) method was used to describe the electron ion interaction.[4, 5] The electron exchange correlation energy was treated within the generalized gradient approximation in the Perdew-Burke-Ernzerhof formalism (GGA-PBE).[6] The calculations were performed

with the cutoff energy of 600 eV and Gaussian electron smearing method with σ = 0.05 eV. Spin-polarization was included in all the structural optimizations. The Brillouin zone integration was calculated using 3×1×2 Monkhorst-Pack *k*-point mesh for a (2×1×2) supercell of γ-FeOOH.[7] It is well known that DFT could not properly handle the strong on-site Coulomb repulsion of the d and f electrons for solid materials. For Fe element, a Hubbard term with U= 5 eV was found to the best compromise for reproducing the experimental band gap of 2.0 eV of the bulk γ-FeOOH.[8] For U element, a Hubbard term with U= 1.9 eV for U(VI) was used as previously,[9] whereas Hubbard term with U = 4.0 eV for UO_2(s).[10] The lattice parameters of γ-FeOOH used here were achieved from high accuracy geometry optimization of a unit cell.[11] The antiferromagnetic arrangement (AFM) was taken into account for γ-FeOOH with antiparallel spin into and between layers in all the calculations. Figure S2 shows the optimized structure of the lepidocrocite (a = 3.05 Å, b = 12.59 Å and c = 3.85 Å), which was agreed very well with the previous study (a= 3.08 Å, b= 12.50 Å and c=3.87 Å).[11] Figure S3 shows three possible binding fashions of U(IV) with orthorhombic lattice of γ-FeOOH, whereas five basically possible positions of U(V) and U(IV) were showed in Figure S4 and S5, respectively.

The required energies (E_{BE}) of uranium (U(IV), U(V) and U(VI)) desorbed from γ-FeOOH were calculated by the differences in the Gibbs free energies of the products and reactants, which can be described by Eqns. (S2-S4):

$$E_{BE} = E_{U^{IV}S_2(H_2O)_5} + E_{FeOOH} - E_{FeOO\text{-}U^{IV}} - 4E_{H^+} - 5E_{H_2O} - 2E_{S^{2-}} \quad (S2)$$

$$E_{BE} = E_{U^{VI}O_2S(H_2O)_4} + E_{FeOOH} - E_{FeOO\text{-}U^{VI}O_2} - 2E_{H^+} - 4E_{H_2O} - E_{S^{2-}} \quad (S3)$$

$$E_{BE} = E_{U^{V}O_2S(H_2O)_4^{-}} + E_{FeOOH} - E_{FeOO\text{-}U^{V}O_2} - E_{H^{+}} - 4E_{H_2O} - E_{S^{2-}} \quad (S4)$$

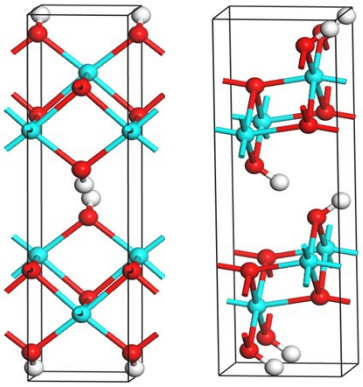

Figure S2 Optimized structure of the lepidocrocite bulk, Red, O; H, grey; Fe, green.

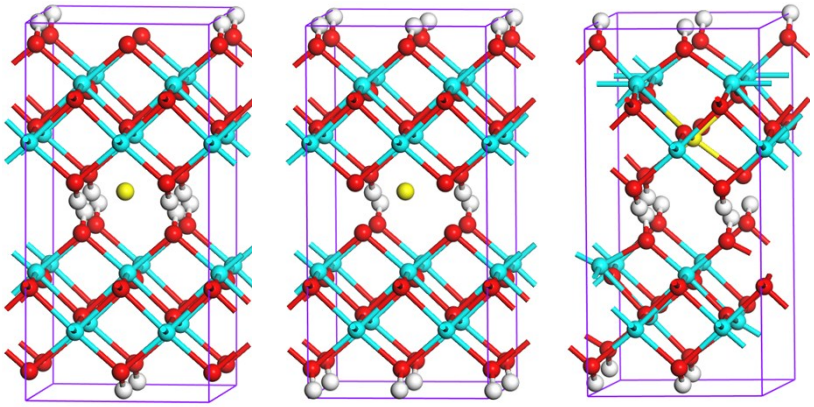

U(IV)-1 **U(IV)-2** **U(IV)-3**

Figure S3 Initial binding modes of U(IV) cations in the initial (2×1×2) supercell of lepidocrocite. Red, O; H, grey; Fe, green; U, blue.

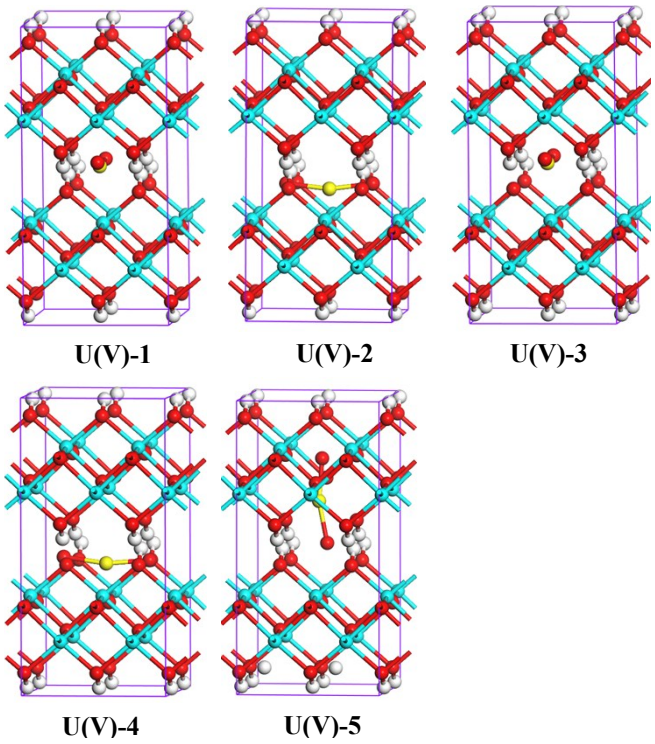

Figure S4 Initial binding modes of U(V) in the initial (2×1×2) supercell of lepidocrocite. Red, O; H, grey; Fe, green; U, blue.

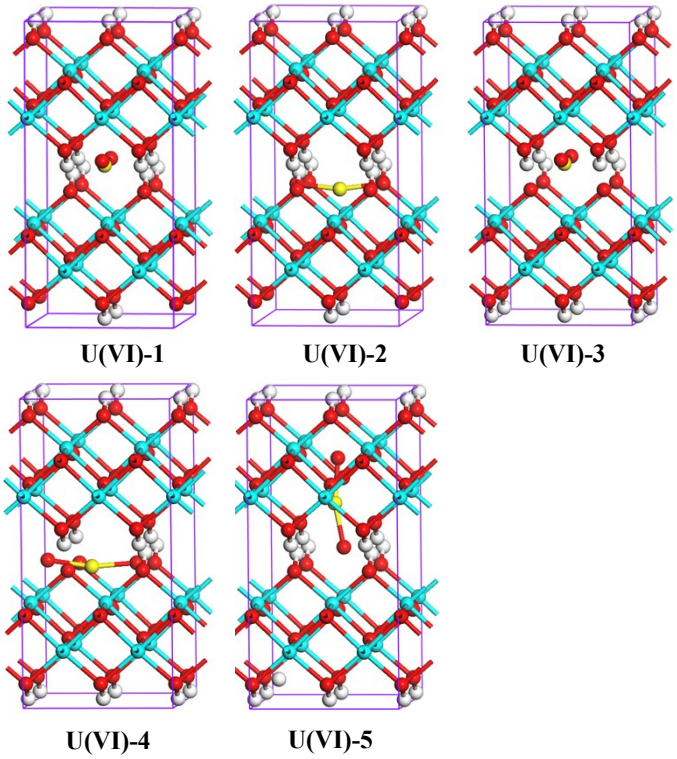

Figure S5 Initial binding modes of U(VI) in the initial (2×1×2) supercell of lepidocrocite. Red, O; H, grey; Fe, green; U, blue.

Table S1 Reaction energies of U(IV), U(V) and U(VI) with lepidocrocite under different binding fashions

Modes	ΔE (kcal/mol)	Reactions
U(IV)-1	-49.56	$FeOO\text{-}U^{IV} + 4H^+ + 5H_2O + 2S^{2-} = U^{IV}S_2(H_2O)_5 + FeOOH$
U(IV)-2	-26.16	
U(IV)-3	-32.97	$FeOO\text{-}U^{IV} + H^+ + Fe(H_2O)_5^{3+} + 2S^{2-} = U^{IV}S_2(H_2O)_5 + FeOOH$
U(VI)-1	-21.12	$FeOO\text{-}U^{VI}O_2 + 2H^+ + 4H_2O + S^{2-} = U^{VI}O_2S(H_2O)_4 + FeOOH$
U(VI)-2	-24.67	
U(VI)-3	-19.13	
U(VI)-4	-18.87	
U(VI)-5	-21.99	$FeOO\text{-}U^{VI}O_2 - H_3O^+ + Fe(H_2O)_5^{3+} + S^{2-} = U^{VI}O_2S(H_2O)_4 + FeOOH$
U(V)-1	-14.16	$FeOO\text{-}U^{V}O_2 + H^+ + 4H_2O + S^{2-} = U^{V}O_2S(H_2O)_4^- + FeOOH$
U(V)-2	-14.17	
U(V)-3	-12.78	
U(V)-4	-13.05	
U(V)-5	-20.51	$FeOO\text{-}U^{V}O_2 - H_2O - 2H^+ + Fe(H_2O)_5^{3+} + S^{2-} = U^{V}O_2S(H_2O)_4^- + FeOOH$
U(V)-1a	-7.54	$FeOO\text{-}U^{V}O_2 + H^+ + 5H_2O = U^{V}O_2(H_2O)_5^- + FeOOH$
U(V)-2a	-7.54	
U(V)-3a	-6.15	
U(V)-4a	-6.42	
U(V)-5a	-13.88	$FeOO\text{-}U^{V}O_2 - 2H^+ + Fe(H_2O)_5^{3+} = U^{V}O_2(H_2O)_5^+ + FeOOH$

Desorption of Fe^{2+} and total Fe (Fe^{2+} and Fe^{3+})

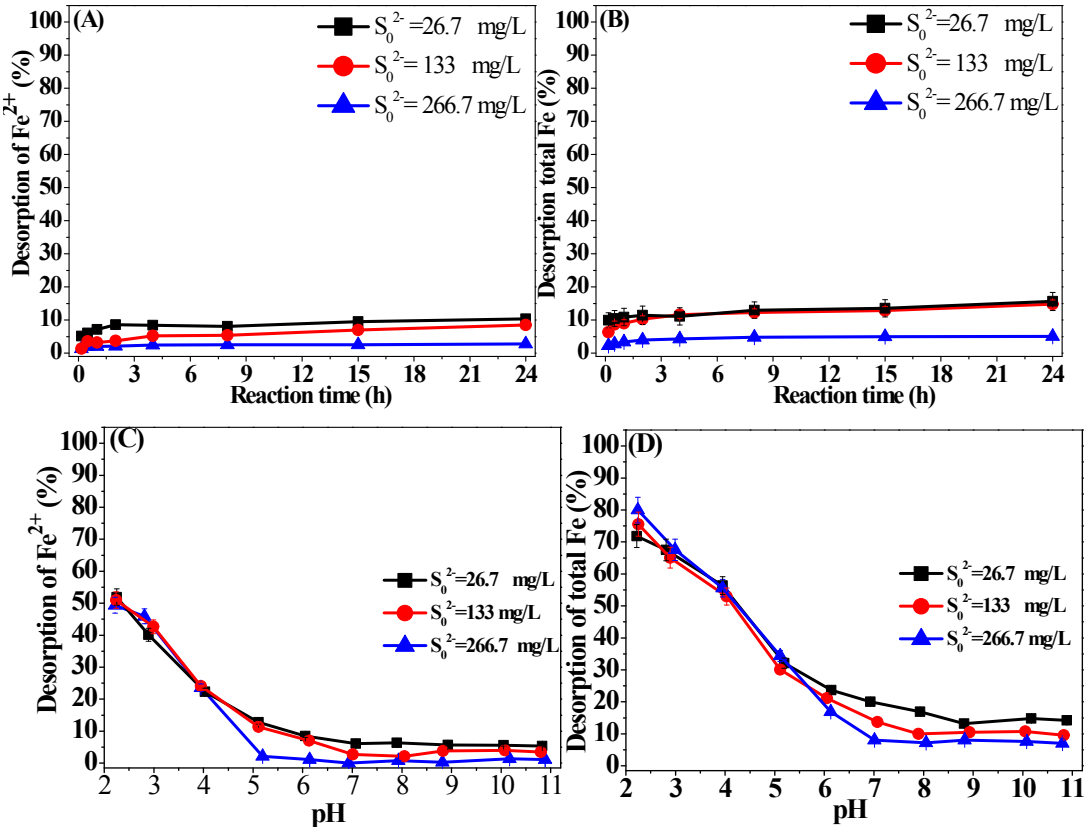

Figure S6. Effect of reaction time (A and B) pH (C and D) on desorption of Fe^{2+} (A and C) and total Fe (B and D) from nano-magnetite under different S^{2-} conditions

Iterative transformation factor analysis (ITFA)

ITFA method has been extensively used for the EXAFS spectra of U(VI).[S12-15] The fraction of the U(VI), U(V) and U(IV) in uranium-bearing sorption samples was calculated by as following steps. Firstly of all, the number of main components for all sorption samples was optimized using principal component analysis (PCA) approach. The EXAFS spectra of sorption samples were reproduced by a linear combination of three components (i.e., U(VI), U(V) and U(IV)). Secondly, iterative target test (ITT) and VARIMAX procedure have been applied to determine the relative concentrations of U(VI), U(V) and U(IV) by assuming UO_2 and UO_3 with 100 % of U(IV) and U(VI),

respectively.

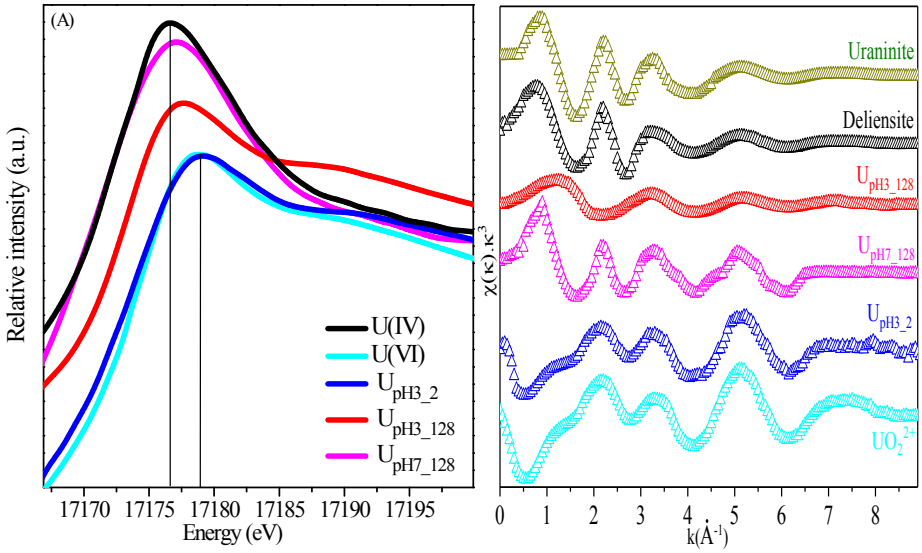

Figure S7 U L_{III}-edge EXAFS spectra of standards (UO_2^{2+}, deliensite and uraninite) and samples (U_{pH3_2}, U_{pH3_128} and U_{pH7_128}).

Table S2 Adsorption (Uads), desorption (Udes) and reduction (Ured) of U, fractions of U(VI), U(V) and U(IV) in U_{pH3_2}, U_{pH3_128} and U_{pH7_128} samples

Sample	U_{ads} (mg/g)	U_{des} (mg/g)	Ured (mg/g)	$U^{(VI)}$ (%)	RE	$U^{(V)}$ (%)	RE	$U^{(IV)}$ (%)	RE
U_{pH3_2}	7.88	6.70	0.18	83.9	0.25	2.5	3.24	13.2	0.53
U_{pH3_128}	7.88	4.65	2.83	12.25	0.65	81.2	2.1	6.3	0.86
U_{pH7_128}	22.10	1.24	19.45	6.68	0.69	7.67	3.54	85.6	0.26

References

1. B. Gu, L. Liang, M. J. Dickey, X. Yin and S. Dai, *Environ. Sci. Technol.*, 1998, 32, 3366-3373.
2. G. Kresse and J. Hafner, *Phys. Rev. B*, 1993, 47, 558-561.
3. G. Kresse and J. Furthmuller, *Phys. Rev. B*, 1996, 54, 11169-11186.
4. P. E. Blochl, *Phys. Rev. B*, 1994, 50, 17953-17979.
5. G. Kresse and D. Joubert, *Phys. Rev. B*, 1999, 59, 1758-1775.
6. J. P. Perdew, K. Burke and M. Ernzerhof, *Phys. Rev. Lett.*, 1996, 77, 3865-3868.

7. H. J. Monkhorst and J. D. Pack, *Phys. Rev. B*, 1976, 13, 5188-5192.
8. H. Guo and A. S. Barnard, *Phys. Rev. B*, 2011, 83, 094112.
9. T. Bo, J.-H. Lan, Y.-J. Zhang, Y.-L. Zhao, C.-H. He, Z.-F. Chai and W.-Q. Shi, *Phys. Chem. Chem. Phys.*, 2016, 18, 13255-13266.
10. S. L. Dudarev, D. N. Manh and A. P. Sutton, *Philos. Mag. B*, 1997, 75, 613-628.
11. H. Christensen and A. N. Christensen, *Acta Chem. Scan.*, 1978, 32, 87-88.
12. V. G. Alexandratos, T. Behrends and P. Van Cappellen, *Environ. Sci. Technol.*, 2017, 51, 2140-2150.
13. I. Pidchenko, K. O. Kvashnina, T. Yokosawa, N. Finck, S. Bahl, D. Schild, R. Polly, E. Bohnert, A. Rossberg, J. Göttlicher, K. Dardenne, J. Rothe, T. Schafer, H. Geckeis and T. Vitova, *Environ. Sci. Technol.*, 2017, 51, 2217-2225.
14. A. Rossberg, T. Reich and G. Bernhard, *Anal. Bioanal. Chem.*, 2003, 376, 631-638.
15. A. Rossberg, K.-U. Ulrich, S. Weiss, S. Tsushima, T. Hiemstra and A. C. Scheinost, *Environ. Sci. Technol.*, 2009, 43, 1400-1406.